Multi-Wavelength View of the Interstellar Medium in the Large Magellanic Cloud

You-Hua Chu

Astronomy Dept., Univ. of Illinois, 1002 W. Green Street, Urbana, IL 61801, USA
chu@astro.uiuc.edu

Abstract

The Large Magellanic Cloud (LMC) has been surveyed in optical emission lines, X-rays, radio continuum, HI, and CO lines. These surveys provide unprecedentedly clear views of the interstellar medium (ISM) in the LMC, allowing us to study astrophysical processes and to examine the relationship among the different phases of the ISM. Multi-wavelength images are used to illustrate the physical structures of supernova remnants, superbubbles, and supergiant shells, as well as the global interstellar structure of the LMC.

Keywords: Magellanic Clouds – galaxies: ISM – ISM: general – ISM: structure – ISM: bubbles – supernova remnants

1 Introduction

The Large Magellanic Cloud (LMC) provides an ideal site for observational studies of the interstellar medium (ISM), as its small inclination (30–40°) minimizes the confusion along the line of sight, its small distance (50 kpc) affords high spatial resolutions, and its small foreground and internal extinctions (typically $A_v < 0.5$ mag) offer unobscured views. Interstellar structures of the LMC can be studied in detail across the entire galaxy.

The ISM exists in multiple phases, including ionized gas at temperatures ranging from 10^4 K to several 10^6 K, neutral atomic gas, and molecular gas. To achieve a comprehensive understanding of the physical structure and evolution of the ISM, one must study all of these components. Interstellar gas in different physical conditions emits preferentially in different wavelength ranges, while the sophistication of observing facilities for these wavelengths has been advancing disparately. It is not until recently that high-resolution radio and X-ray images of the LMC have become available. We are finally able to examine the multiple-phase ISM of the LMC at multiple wavelengths in great detail.

2 Multi-Wavelength Observations of the Multi-Phase ISM

A variety of observing facilities have been used to study the multi-phase ISM of the LMC. For the 10^4 K ionized gas, emission-line images were taken with a CCD camera on the Curtis Schmidt telescope at Cerro Tololo Inter-American Observatory (CTIO), and long-slit high-dispersion spectra were taken with the echelle spectrograph on the CTIO 4m telescope. The emission-line (Hα, [O III], and [S II]) images show the distribution and excitation of the ionized gas (Smith et al. 1997), while the echelle spectra show the internal motion and shocks in the ionized gas (e.g., Chu & Kennicutt 1994).

The 10^5 K ionized gas has been studied with interstellar absorption line observations in the UV, using C IV $\lambda\lambda$1548,1550, Si IV $\lambda\lambda$1393,1402, and N V $\lambda\lambda$1238,1242 lines. A large number of high-dispersion spectra of early-type stars in the LMC are available in the International Ultraviolet Explorer archives. These spectra are useful in diagnosing shocks inside superbubbles or supergiant shells, but provide no information on the hot gas halo of the LMC (Chu et al. 1994). The Goddard High Resolution Spectrograph (GHRS) on-board the Hubble Space Telescope (HST) has been used to take high-dispersion spectra with high S/N. With a careful selection of cool probe stars in quiescent interstellar environments, it is possible to determine not only the column density but also the kinematics of the 10^5 K gas halo of the LMC (Wakker et al. 1997).

The 10^6 K ionized gas is best observed in soft X-rays. The ROSAT X-ray satellite provides two detectors: the Position Sensitive Proportional Counter (PSPC) and the High Resolution Imager (HRI). The PSPC, sensitive to 0.1–2.4 keV, has an on-axis angular resolution of $\sim 30''$ and a spectral resolution of 45% at 1 keV. The HRI, sensitive to 0.1–2.0 keV, has an on-axis resolution of $\sim 5''$, but has essentially no spectral resolution. Both the PSPC and the HRI have been used to survey the LMC (Snowden & Petre 1994; Chu, Snowden, & Chang 1996).

The HI distribution in the LMC has been mapped with the Parkes 64m telescope at an angular resolution of $\sim 15'$ (Rohlfs et al. 1984). An HI mosaic of the LMC has recently been obtained with the Australia Telescope Compact Array (ATCA) at a resolution of $1'$ (Kim et al. 1997a).

The molecular gas in the LMC has been mapped at a resolution of $8\farcm8$ in the $J = 1 \rightarrow 0$ rotational transition of CO (Cohen et al. 1988). A more recent CO survey of the LMC was carried out with the Swedish-ESO Submillimeter Telescope (SEST) at a resolution of $45''$ (Israel et al. 1993). The SEST CO maps of two star-formation regions, 30 Dor and N11, have been presented by Caldwell & Kutner (1996).

3 Structures of the Interstellar Medium in the LMC

The structure of the ISM is determined by the interplay between massive stars and the ISM: molecular clouds form massive stars; massive stars dissociate, ionize, and dynamically structure the ambient medium; the ionized medium eventually cools, recombines, contracts under gravity, and forms molecular clouds. This simplistic picture can qualitatively explain the dramatically different structures of the ionized and neutral interstellar components in the LMC.

The structure of the molecular ISM in the LMC can be seen in the low-resolution CO map presented by Cohen et al. (1988). The large molecular concentrations are usually the sites of star formation activities. The most intense star formation region, the 30 Dor complex, sits on the northern tip of the largest and most massive concentration of molecular gas. In high-resolution maps of star forming regions, such as N11 (Caldwell & Kutner 1996), remnant molecular gas is present and associated with the densest compact HII regions.

The structure of the neutral atomic ISM in the LMC is revealed in detail in the ATCA HI mosaic (Kim et al. 1997a). The differences between this ATCA mosaic and the Parkes 64m map (Rohlfs et al. 1984) are clearly caused by the difference in resolution; however, the absence of a prominent HI ridge to the south of 30 Dor in the ATCA map might be indicative of a "missing short baseline" problem, which prohibits the detection of wide features. The ATCA image, reproduced in the left panel of Figure 1, is dominated by HI filaments with interspersed holes across the entire galaxy. Hardly any correspondence between the HI features and distributions of stars or other

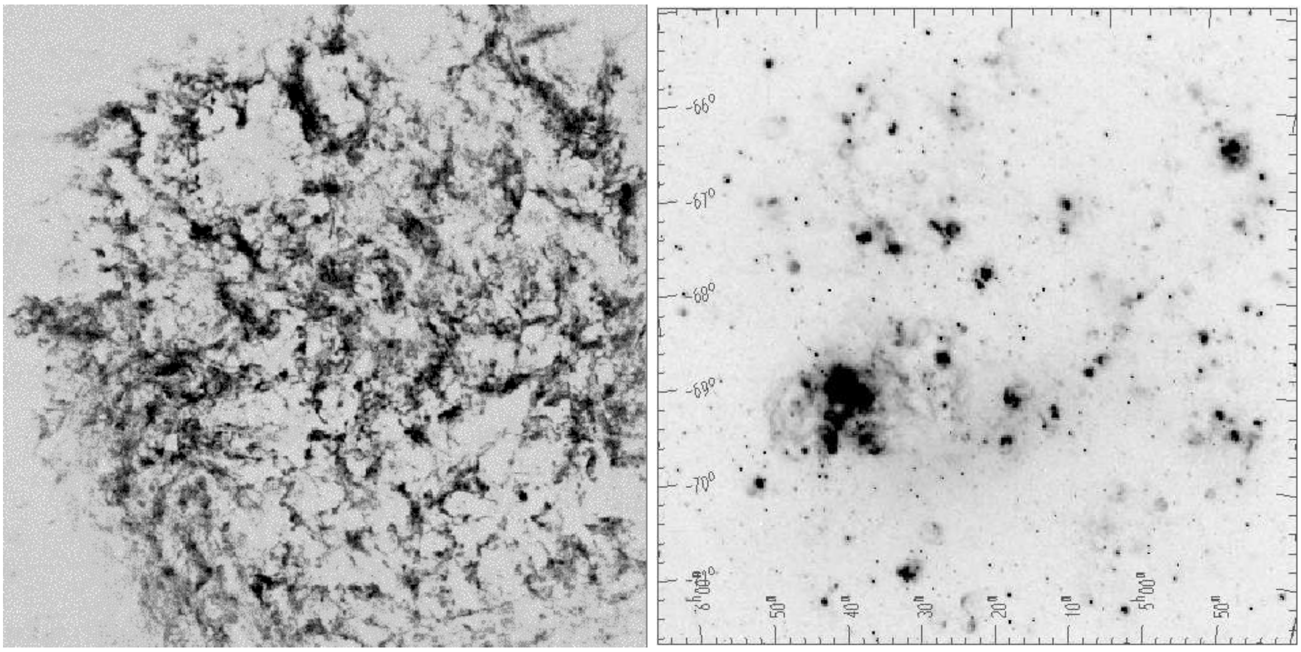

Figure 1: HI (left) and Hα (right) images of the LMC.

components of the ISM are obvious, besides the HI cavities in the supergiant shells (SGSs) LMC 4 and LMC 5 (Kim et al. 1997a).

It is conceivable that the HI map should show a complex filamentary structure because it represents the cumulative effects of dynamic interactions of massive stars with the ISM in the past. If the HI maps are displayed with velocity resolution (in channel maps), correspondence between HI holes and ionized gas shells may become clear (Kim et al. 1997b).

The structure of the 10^4 K ionized interstellar gas is well depicted by Hα images, which can be obtained with high resolution ($\sim 1''$) easily. The Hα image of the LMC displayed in the right panel of Figure 1 shows prominent HII regions, SGSs with sizes up to $\sim$1400 pc, and diffuse gas that contributes up to 30–40% of the total Hα emission of the LMC (Kennicutt et al. 1995). The 10^4 K ionized gas is closely associated with massive stars. Massive stars are responsible for not only the ionization of the medium, but also the dynamic structuring of the medium via fast stellar winds and supernova ejecta. Massive stars have short lifetimes, hence the structure of the 10^4 K ionized ISM is freshly minted within the last 10^7 yrs. It is thus not surprising that the Hα and the HI images of the LMC (Figure 1) look so different.

Examined closely, the 10^4 K ionized gas often show shell structures in supernova remnants (SNRs) and shell HII regions around OB associations (superbubbles). The top panel of Figure 2 shows an Hα image of a portion of the LMC centered near the 30 Dor complex; the SGSs LMC 2 and LMC 3, the superbubbles in the HII regions N158 and N160, and the large shells of SNRs DEM299 and DEM316 are clearly visible.

The 10^6 K ionized gas is produced dynamically by fast stellar winds from massive stars or supernova ejecta. It is thus expected that some correspondence between the 10^6 K ionized gas and the 10^4 K ionized gas exists. Indeed, Figure 2 shows that the 10^6 K ionized gas, as traced by soft X-ray emission, is detected in the interiors of SGSs, superbubbles, and SNRs, which have been identified by their HII shells. The X-ray emission from the SGS LMC 4 has been analyzed by Bomans et al. (1994); X-ray emission mechanisms for superbubbles have been summarized by Chu & Mac Low (1996); a multi-wavelength study of the SNR DEM316 has been reported by Williams et al. (1997).

The relationship between the 10^4 K ionized gas and the 10^6 K ionized gas and the production of the 10^6 K gas by shocks are demonstrated in Figure 3, the central $9' \times 9'$ of 30 Doradus. It is evident that the bright diffuse X-ray emission is closely correlated with the presence of high-velocity, shocked material detected in the Hα echellograms.

On large scales, the distribution of the 10^6 K gas show features whose origin is not very clear. For example, the LMC bar contains only a few scattered HII regions, but it displays bright diffuse X-ray emission. Another example is the bright X-ray spur extending to the south of the supergiant shell LMC 2; no optical counterpart is known or detected. The on-going ROSAT HRI survey of the LMC will provide high-resolution X-ray images and may help clarify the origin of this hot gas.

Finally, a 10^5 K gas halo of the LMC has been unambiguously detected by Wakker et al. (1997) using HST GHRS observations of five probe stars. They find the hot gas halo to be patchy and expanding outward relative to the warm ionized gas (seen in Hα) in the disk. Observations along more sightlines are needed to confirm these results and to determine the relationship between the 10^5 K halo gas and the 10^6 K hot gas readily visible in soft X-ray images.

Acknowledgements

YHC would like to thank R.C. Smith and R.C. Kennicutt for providing the Hα images, S. Kim and L. Staveley-Smith for the HI 21-cm mosaic, and S. L. Snowden for the ROSAT PSPC and HRI mosaics of the LMC. YHC acknowledges the support of NASA grants NAG 5-1900, NAG 5-3246, STI5787.01-94A, STI5894.02-94A, and STI6122.01-94A.

References

Bomans, D.J., Dennerl, K., & Kürster, M. 1994 A&A, 283, L21

Caldwell, D.A., & Kutner, M.L. 1996 ApJ, 472, 611

Chu, Y.-H. 1995 RevMexAA (Conference Series), 3, 153

Chu, Y.-H., & Kennicutt, R.C. 1994 ApJ, 425, 720

Chu Y.-H. & Mac Low M.-M. 1996 in "Röntgenstrahlung from the Universe", ed. H.U. Zimmermann, J.E. Trümper, and H. Yorke, 241

Chu, Y.-H., Snowden, S.L., & Chang, T. 1996 The ROSAT Newsletter, No. 13, p. 26

Chu, Y.-H., Wakker, B., Mac Low, M.-M., & García-Segura, G. 1994 AJ, 108, 1696

Cohen, R.S., Dame, T.M., Garay, G., et al. 1988 ApJ, 331, L95

Davies, R.D., Elliott, K.H., & Meaburn, J. 1976 MemRAS, 81, 89

Henize, K.G. 1956 ApJS, 2, 315

Israel, F.P. et al. 1993 A&A, 276, 25

Kennicutt, R.C., Bresolin, F., Bomans, D.J., Bothun, G.D., Thompson, I.B. 1995 AJ, 109, 594

Kim, S., Staveley-Smith, L., Sault, R.J., Kesteven, M.J., McConnell, D., & Freeman, K.C. 1997a PASA, 14, (April issue, in press)

Kim, S., Chu, Y.-H., Staveley-Smith, L., & Smith, R.C. 1997b submitted to ApJ

Mathewson, D.S., Ford, V.L., Dopita, M.A., et al. 1983 ApJS, 51, 345

Rohlfs, K., Kreitschmann, J., Siegman, B.C., & Feitzinger, J.V. 1984 A&A, 137, 343

Smith, R.C., et al. 1997, in this volume (MCELS)

Snowden, S.L., & Petre, R. 1994 ApJ, 436, L123

Wakker, B., Howk, J.C., Chu, Y.-H., Bomans, D., & Points, S. 1997, submitted to ApJ

Williams, R.M., Chu, Y.-H., Dickel, J.R., Beyer, R., Petre, R., Smith, R.C., Milne, D.K. 1997 ApJ, 480, 618

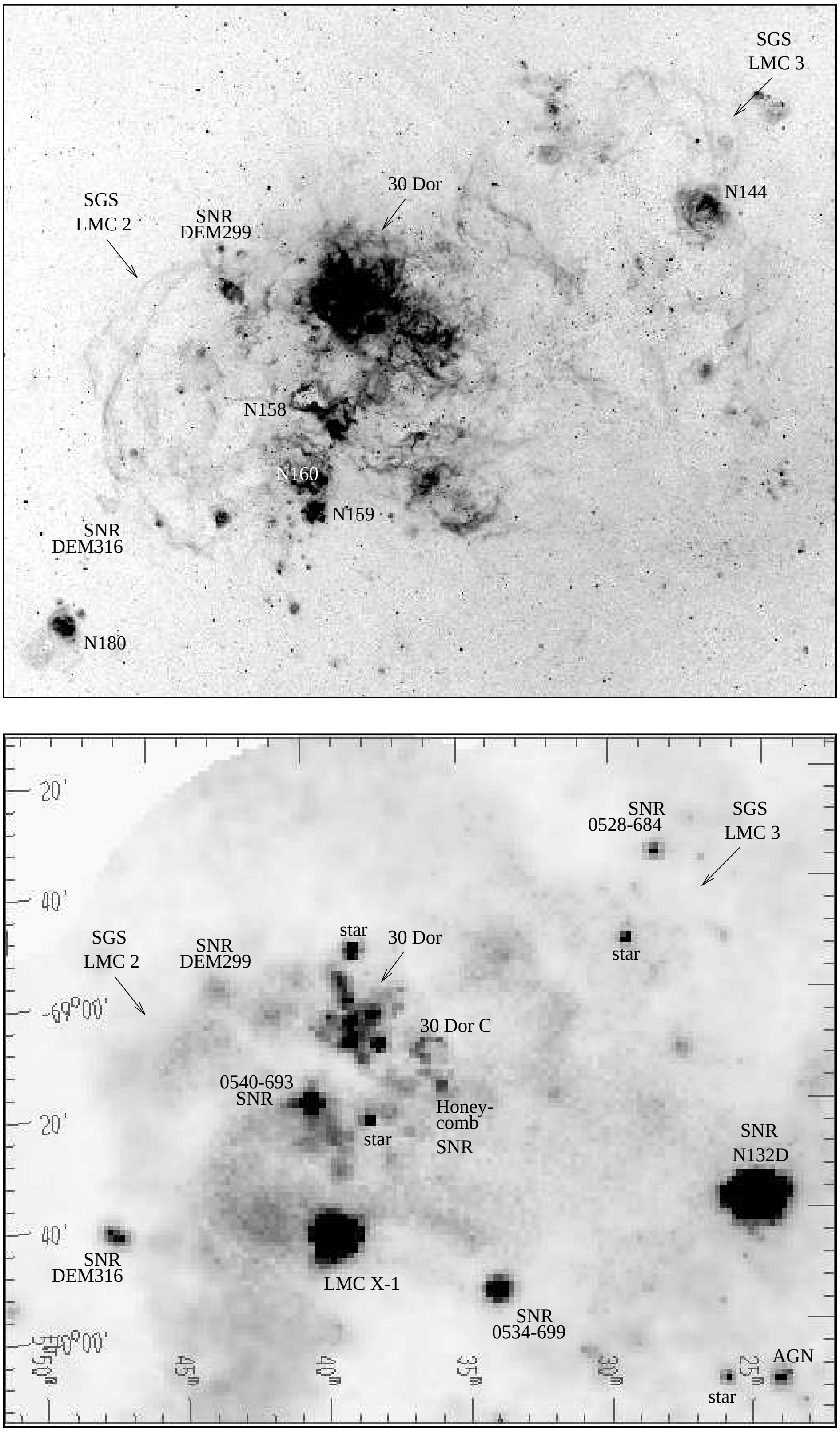

Figure 2: Hα (top) and X-ray (bottom) images of a portion of the LMC centered near the 30 Dor complex. Bright HII regions, supernova remnants (SNRs), and supergiant shells (SGSs) are labeled. The HII region and SNR names are from Henize (1956, "N"), Davies, Elliott, & Meaburn (1976, "DEM"), and Mathewson et al. (1983).

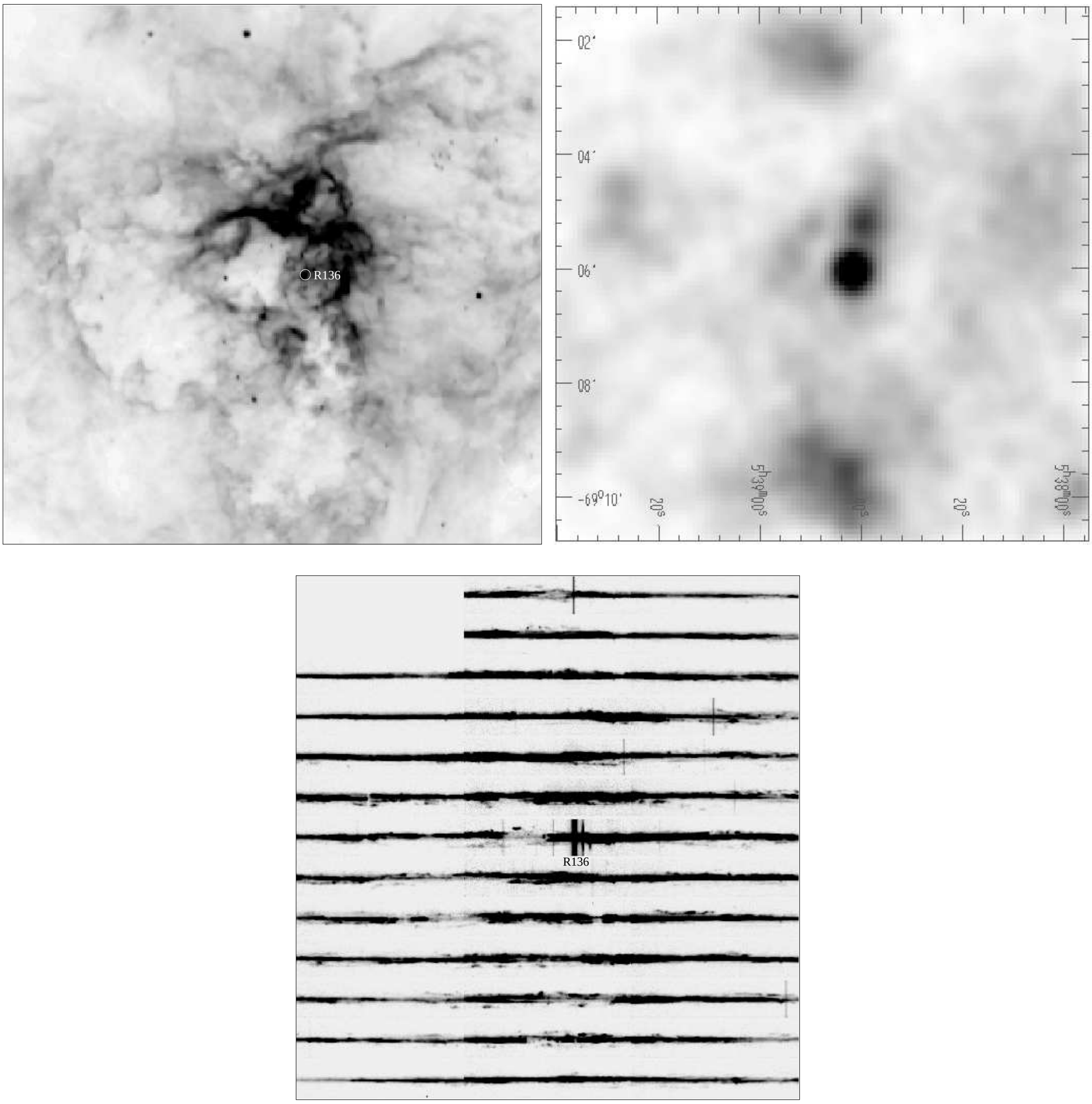

Figure 3: Hα (top left) and X-ray (top right) images of the central $9' \times 9'$ of 30 Doradus. The X-ray image is extracted from a ROSAT PSPC observation in the 0.1–2.4 keV band. The bottom panel contains long-slit Hα echellograms of the same region, reproduced from Chu & Kennicutt (1994). The wavelength increases upwards. The orientation is the same as the images above. The separation between adjacent slits corresponds to $45''$ in the sky or 600 km s^{-1} in velocity.